

# SPATIOTEMPORAL DYNAMICS AND SIMULATION OF THE THERMAL FUSING PROCESS IN ELECTROPHOTOGRAPHIC PRINTING

Stephan Studener<sup>1</sup>, Boris Lohmann<sup>1</sup>

<sup>1</sup>Technische Universität München, Germany

Corresponding author: Stephan Studener,  
Institute of Automatic Control / Faculty of Mechanical Engineering  
Technische Universität München  
85748 Garching bei München, Boltzmannstr. 15 - Germany  
stephan.studener@tum.de

**Abstract.** In this contribution a model for the spatiotemporal dynamics of the thermal fusing process in electro photographic printing is derived. The model is a dynamical system consisting of two hyperbolic partial differential equations (PDEs) for the temperature and moisture content of the paper web. In the following the Method of Characteristics and the geometrical interpretation of a first order PDE is employed as a vital tool to simulate different control strategies with high accuracy and determine the state of the paper web during launching of the printing machine and transient steps in the process.

## 1 Introduction

Xerographic images are composed of numerous toner particles deposited on well defined locations on paper by control of adhesive forces. When the toner is first transferred from the photo conductor to paper, it adheres to the paper fibers because of electrostatic and dispersion forces [5, 11]. In this condition the image is easily rubbed off by the slightest contact with another surface, so the image must be fixed permanently to the paper substrate. In the process at hand the toner is fused to the paper and the energy required for this thermal activated process is transferred to the surface by radiation. Due to events taking place further upstream, the fusing process cannot be operated continuous, in fact the way of processing is semi-batch: A certain amount of paper is carried through the domain at a constant pace, before the process stops. During the break, already fused paper elements are drawn back into the machine. At the end of the break, the paper web is accelerated in the direction of processing and finally the velocity returns to a constant pace and the process operates at steady state until the next break is required [5].

The contribution is separated into two parts: i) The deviation of a process model and ii) the presentation of a method for simulation, which is tailored for nonlinear, time variant transport processes such as the thermal fusing process in electro photographic printing.

First the modeling procedure is taken into consideration. A process model is required as a basis for simulation, identification and evaluation of different control strategies. A model will be derived from first principles, here the conservation of energy and the conservation of mass. Particular attention is given to the different mechanisms of heat transfer and mass transfer dominating the process, especially the evaporation of water, which is found in the capillaries of the paper web, and the radiant intensity of the emitting surfaces, which depends on the spatial variable [1, 6]. Once a model has been derived the steady state solution will be studied and a set-point or control objective formulated. Matters are complicated by the fact that the parameters are not lumped, but distributed in the system's domain. The resulting model consists of two hyperbolic partial differential equations (PDEs). From the control engineers point of view, the process is a distributed parameter system with the action of the manipulated variables not taking effect on the boundary conditions, but being distributed in the domain. Furthermore the coefficient of the spatial differential operator, namely the process velocity, depends on time. This fact poses difficulties for the design of a controller as well as for simulation of the process: The deviation from the steady state process velocity is of an extend, s. t. a linearization can not longer be justified.

In the second part of the paper a method for simulation of the nonlinear transport equations is presented, which is capable of dealing with time varying coefficients in the main part of the PDEs. Dynamical systems described by hyperbolic PDEs have some characteristic properties which are desired to be preserved in simulation of the process. First, their impulse response settles in a finite time. Secondly the eigenvalues of the spatial modes of the spatial differential operator cluster at minus infinity, which essentially means that each mode contributes an equal amount of energy to the impulse response [2]: Reducing the order of the system by neglecting fast modes is impossible. This is the reason why simulation methods, that have become the industrial standard, like Discretization on Finite Elements, Finite Differences or Finite Volumes do not predict the evolution of the system satisfactorily: Lumping of the parameters leads to a finite dimensional system whose impulse response settles in infinite time and whose poles are distinguishable from each other. Thus the lumped parameter system has slow and fast parts that may be neglected. Since the process velocity can vary in sign, large difficulties are encountered even if one wants to apply Discretization on Finite Volumes, a lumping technique suitable for transport processes: At some point in time the boundary condition on a different part of the domain must be provided. To overcome the difficulties arising

with discretization and preserve the characteristic dynamics of the system, the Method of Characteristics and the geometrical interpretation of a first order PDE is applied to simulate the plant output and the distribution of the state variables in the domain [3]. It will be shown, that this method preserves the characteristic dynamics of the system and does require less numerical effort than classical lumping techniques. To illustrate the effectiveness of the simulation method, the current control configuration of the plant is simulated and as a part of the conclusions, based on the prediction of the model, possible improvements are discussed.

## 2 Conservation of Mass and Energy

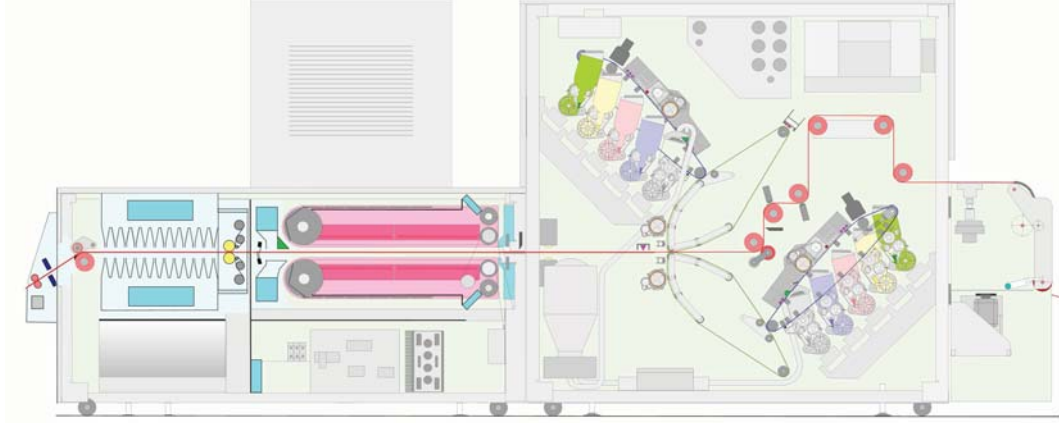


**Figure 1:** The electro photographic printing process. From left to right: Cooling of the paper web, fusing of the toner and deposition of the particles. The paper web is displayed as a red band being guided and transported through the process by rolls. The steady state direction of processing is from right to left.

In the following thermodynamical aspects of the fusing process are taken into consideration. The process is schematically displayed in figure 1. The quality of the fused image is determined by the adhesive forces generated between paper and particles and the gloss of the image. Both are physical quantities, which depend on the temperature of the paper web. Experience shows, that the quality of the fused image is satisfying, if each (differential) paper element leaves the fusing apparatus with a desired outlet temperature. Since paper is a hygroscopic matter, it contains water, which is evaporated during the fusing process. The energy required to evaporate water, which is found in the capillaries of the paper web, must be transferred to the web by convective and radiant heat transfer. This process cannot be avoided and the evaporation of water thus becomes a sink of energy and mass. In order to obtain equations describing the fusing process, the first law of thermodynamics is applied to a differential control volume found at an arbitrary location in the fusing apparatus. The thickness of the web  $d_P$  is much smaller than its length and with, thus conduction of heat in this direction can be neglected. Conservation of energy applied to the control volume yields:

$$\rho_P \cdot c_P \cdot \frac{\partial T}{\partial t} = \lambda_P \cdot \left( \frac{\partial^2 T}{\partial z_1^2} + \frac{\partial^2 T}{\partial z_2^2} \right) - v(t) \cdot \rho_P \cdot c_P \cdot \frac{\partial T}{\partial z_1} - \frac{2 \cdot \alpha}{d_P} \cdot (T - T_\infty(t, z_1, z_2)) + \sum_{i=1}^{12} \frac{2 \cdot \varepsilon}{d_P} \cdot f_{VF,i}(z_1, z_2, u) \cdot (T_{E,i}^4 - T^4) - \frac{2 \cdot \beta \cdot \rho_P}{d_P} \cdot (X - X^*(T)) \cdot \Delta H_{Evap} \quad (1)$$

The first term on the RHS of the above equation describes conductive heat transfer in accordance with Fourier's Law and the second one denotes the amount of heat being transported through the domain with velocity  $v(t)$ . Since the Peclet-Number  $Pe = v_s \cdot L \cdot \rho_P \cdot c_P \cdot \lambda^{-1}$ , with the steady state process velocity  $v_s$ , is much larger than 1,  $Pe \gg 1$ , conduction can be neglected. The third term on the RHS denotes convective heat exchange with the environmental temperature  $T_\infty(t, z_1, z_2) \approx T_\infty(z_1)$ ,

$$T_\infty(z_1) = \begin{cases} T_0, & z < 0 \\ T_{env}, & 0 \leq z \leq L \\ T_0, & z > L \end{cases} \quad (2)$$

in different subdomains. Inside the fusing apparatus the environmental temperature is equal to  $T_{env}$ ; before this step in the printing process and inside the the cooling  $T_\infty(z_1) = T_0$ . The amount of heat exchanged depends on  $\alpha$ , the transfer coefficient. It is assumed to depend on the process velocity, as derived in [1, 6]. The amount of radiant energy being exchanged with emitting surfaces having the temperature  $T_{E,i}$  is described by the fourth term on the RHS.  $f_{VF,i}(z_1, z_2, u)$  is the viewfactor of the differential element. It can be derived from the relative orientation of both the emitter surface  $i$  and the location of the differential paper element [7]. The emitters are arranged as shown

in figure 2 at a distance  $H$  above and below the web. The view factor is given by the following integral:

$$f_{VF,i}(z_1, z_2, u) = \int_{S_{Emitter,i}(u)} \int \left( \frac{H}{H^2 + (z_1 - z_{E,1})^2 + (z_2 - z_{E,2})^2} \right)^2 dz_{E,1} dz_{E,2} \quad (3)$$

$S_{Emitter,i}(u)$  is the surface of the emitter  $i$ . A closed form of the solution does not exist and the integral must be evaluated by numerical quadrature. The emitting surfaces can be covered by a curtain, which implies, that, depending on how far the curtain is opened, their viewfactor takes different values.  $u$  is the length of the emitting surfaces, that is uncovered (see figure 2).  $\varepsilon$  is the emission coefficient and is assumed to be constant for all emitting surfaces.  $\varepsilon$  is determined using the following formula:

$$\varepsilon = \sigma \cdot \frac{\varepsilon_P \cdot \varepsilon_E}{1 - (1 - \varepsilon_E) \cdot (1 - \varepsilon_P)} \quad (4)$$

which is derived by tracing a ray that is sequently absorbed and reflected at the paper and emitter surface [7].  $\varepsilon_P$  and  $\varepsilon_E$  are the emission coefficients of the paper surface and the emitter respectively. Note that the emission coefficient  $\varepsilon_P$  depends on the image to be printed: Different colours and most of all the particle population density on the web have large effects on this coefficient. Note that the viewfactor is equal to zero everywhere outside the fusing apparatus. The viewfactors are bell-shaped surfaces and can be interpreted as the density of energy arriving at the surface of the paper web as a function of the spatial variables  $z_1, z_2$  and the position of the curtain  $u(t)$ .

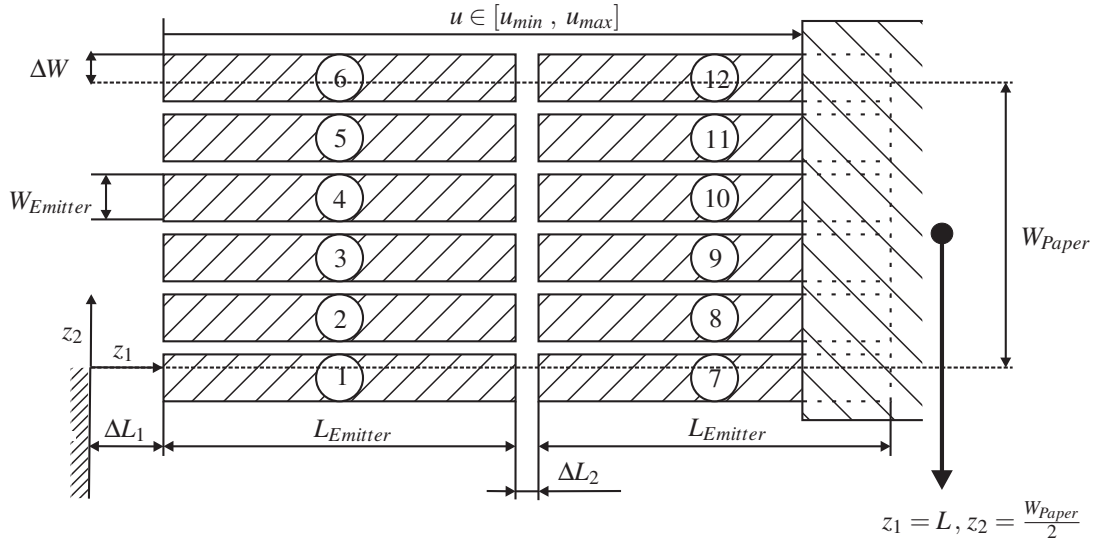


**Figure 2:** Configuration of emitters and paper surface inside the fusing apparatus. The location of the sensor is found at the end of the apparatus and the at the center of the paper web,  $z_{1,out} = L$  and  $z_{2,out} = W_{Paper}/2$ . When  $u = u_{min} = 0$ , the emitters are completely covered by the curtain and exchange of radiant energy with the emitting surfaces is impossible. When  $u = u_{max}$ , the emitters are completely exposed.

The last term of the RHS of the PDE describes how much energy is consumed by the evaporation of water. The amount of water evaporated is proportional to the difference between the current moisture content  $X$  and the equilibrium moisture content  $X^*(T)$ , which depends on the temperature. Instead of moles, in industrial drying it is usual to use the load  $X$  which has units of  $[kg]$  water per  $[kg]$  paper [9]. The equilibrium moisture content is approximated as follows [8]:

$$X^*(T) = X_0 \cdot \exp(-A \cdot (T - T_0)) \quad (5)$$

The energy consumed by evaporation of water is simply the product of the amount of water evaporated and the enthalpy of evaporation  $\Delta H_{Evap}$  [9]. A mass balance applied to the differential control volume results in the following PDE for the moisture content of the paper web:

$$\frac{\partial X}{\partial t} = D \cdot \left( \frac{\partial^2 X}{\partial z_1^2} + \frac{\partial^2 X}{\partial z_2^2} \right) - v(t) \cdot \frac{\partial X}{\partial z_1} - \frac{2 \cdot \beta}{d_p} \cdot (X - X^*(T)) \quad (6)$$

The first term on the RHS of the above PDE denotes diffusive transport of moisture inside the web and the second one denotes transport of moisture due to processing of the paper web with velocity  $v(t)$ . The last term on the RHS of the above equation describes, how much moisture is discharged or taken up due to the difference between equilibrium moisture content  $X^*$  and moisture content  $X$  at the position  $z_1, z_2$  and point in time  $t$ . The mass flow is proportional to a transfer coefficient  $\beta$ . Since the Bodenstein-Number  $Bo = v_s \cdot L \cdot D^{-1}$  is much larger than 1,  $Bo \gg 1$ , diffusion of water can be neglected. Choosing  $z := z_1, x_1 := T, x_2 := X, u_0 := u, u_i := T_{E,i}$  and  $d := T_\infty(z_1)$

and after neglecting diffusive heat and mass transfer, one finally arrives at the following nonlinear, time variant system of first order PDEs:

$$\begin{aligned} \frac{\partial x_1}{\partial t} + v(t) \cdot \frac{\partial x_1}{\partial z} &= \alpha \cdot (d(z) - x_1) + \sum_{i=1}^{12} \varepsilon \cdot f_{VF,i}(z, z_{2,out} u_0) \cdot (u_i^4 - x_1^4) - \beta \cdot (x_2 - X^*(x_1)) \cdot \frac{\Delta H_{Evap}}{c_P} \\ \frac{\partial x_2}{\partial t} + v(t) \cdot \frac{\partial x_2}{\partial z} &= -\beta \cdot (x_2 - X^*(x_1)) \end{aligned} \quad (7)$$

$z \in \mathbb{R}$ ,  $t \in [0, \infty)$  denotes the spatial variable and time,  $\mathbf{x} = [x_1 \ x_2] \in \mathbb{H}[\mathbb{R}, \mathbb{R}^2]$  denotes the state vector functions;  $\mathbb{H}$  is an infinite dimensional Hilbert space of 2-dimensional vector functions defined on  $\mathbb{R}$ . Note that the process parameters  $\alpha$ ,  $\varepsilon$ ,  $\beta$  have been rewritten for the sake of convenience. The viewfactor is evaluated with  $z_1 = z$  and the output location  $z_2 = z_{2,out} = W_{Paper}/2$ . At  $z = -\infty$  the temperature and moisture content of the paper web is equal to  $T_0$  and  $X_0$  respectively. The initial distribution of temperature and moisture content is equal to

$$x_1(t=0, z, z_{2,out}) = g_1(z) \quad x_2(t=0, z, z_{2,out}) = g_2(z) \quad (8)$$

The plant output is given by

$$y(t) = x_1(t, z = L, z_2 = z_{2,out}) \quad (9)$$

**Remark.** By neglecting diffusive heat and mass transfer the second order system of partial differential equations has been reduced to a first order system, in which  $z_2$  is a parameter appearing in the viewfactor only. One is primarily interested in the distribution of temperature in the direction of processing at the sensor location, because that particular temperature is fed back to the control algorithm. Thus one arrives at a hyperbolic distributed parameter system with the states  $x_1$ ,  $x_2$  being distributed in one space dimension. The second spatial variable  $z_2$  is only a parameter, that may be varied. As a consequence, in the model, no heat is exchanged between neighbouring points, only transport in the  $z_1 = z$ -direction occurs. In the following  $z_2$  is dropped and  $\mathbf{x}(t, z, z_2) := \mathbf{x}(t, z)$ ,  $y(t) = x_1(t, z = L)$ .

### 3 Method of Characteristics

The Method of Characteristics is a solution method for first order PDEs which is built on the geometric interpretation of the underlying equations [3]. For purpose of illustration consider the following scalar PDE with boundary and initial conditions

$$\partial_t \cdot x + v(t) \cdot \partial_z \cdot x - f(x, z, t) = 0 \quad x(t=0, z) = g(z), \quad x(t, z=0) = x_b(t) \quad (10)$$

$z \in \Omega \subseteq \mathbb{R} = [0 \ L]$ ,  $t \in [0, \infty)$  and  $x \in \mathbb{H}[\Omega, \mathbb{R}]$ . The PDE can be rewritten as follows:

$$\begin{bmatrix} 1 & v(t) & f(x, z, t) \end{bmatrix} \cdot \begin{bmatrix} \partial_t \cdot x \\ \partial_z \cdot x \\ -1 \end{bmatrix} = 0 \quad (11)$$

These two vectors are orthogonal to each other since their scalar product is equal to zero. The solution of the PDE can be interpreted as a surface in the space spanned by the independent variable  $x$  and the independent variables  $t$  and  $z$ . The solution is  $x = x(t, z)$ . Now consider the function  $F(x, t, z) = x(t, z) - x = 0$ . The gradient of this function is  $\nabla \cdot F = [\partial_t \ \partial_z \ \partial_x]^T \cdot F = [\partial_t \cdot x \ \partial_z \cdot x \ -1]^T$ . Using this result, one finds, that the following must be true

$$\begin{bmatrix} 1 & v(t) & f(x, z, t) \end{bmatrix} \cdot \nabla \cdot F = 0 \quad (12)$$

Since the gradient of  $F$  is normal to the graph of  $F$  in each point in the solution surface, from the equation above one concludes that the vector  $\begin{bmatrix} 1 & v & f(x, z, t) \end{bmatrix}$  must be tangent to  $F$ . Now one can search for curves called the Characteristic Curves  $\mathcal{C} = [t(s) \ z(s) \ x(s)]$ , parametrized by  $s \in I \subseteq \mathbb{R}$ , whose tangent in each point coincides with the vector  $\begin{bmatrix} 1 & v(t) & f(x, z, t) \end{bmatrix}$ . The tangent of the curve must thus be equal to

$$\frac{dt}{ds} = 1 \quad \frac{dz}{ds} = v(t) \quad \frac{dx}{ds} = f(x, t, z) \quad (13)$$

Since  $ds = dt$ , the Characteristic Curves can be directly parametrized by time  $t$ . A point in the solution surface  $x = x(t, z)$  can be found by integrating the set of ordinary differential equations (ODEs) above with appropriate initial conditions, which are  $z(t=0) = z_0$  and  $\mathbf{x}(t=0) = \mathbf{g}(z_0)$ . The thermal fusing process is described by a set of two coupled PDEs, both having the same main part. The characteristic ODEs associated with that set of PDEs are

$$\frac{dt}{ds} = 1 \quad \frac{dz}{ds} = v(t) \quad \frac{d\mathbf{x}}{ds} = \mathbf{f}(\mathbf{x}, z, t) \quad (14)$$

The projection of the Characteristic Curves into the  $[t \ z]$ -plane are the solutions to the first two of the above set of ODEs and can be interpreted as the solution of the equation of motion for a differential element. As an example, the trajectories of a certain number of the  $\infty$  many points traveling through the domain of interest in the thermal fusing process are display in figure 3. The fact that the state of each point can be tracked by integrating the characteristic ODEs with appropriate initial conditions implies that each point evolves in time completely decoupled from neighboring points. This is the case when pure transport through the domain occurs. The time required for the impulse response to settle is equal to the time required for that one point traveling through the domain which can be found at  $z = 0$ , when  $t = t_0$ , the point in time when the impulse is applied. This property is reflected by the Method of Characteristics. By Discretization of the transport equations on Finite Elements, Volumes or Differences a connectivity between neighboring points is introduced, which is not present in the underlying equations. Hence, the characteristic dynamics of hyperbolic dynamical systems are lost due to lumping of the parameters.

## 4 Characteristics Based Simulation of Hyperbolic Plants

Using the proposed method, the output of the plant as well as the distribution of the state variables in the domain will be simulated. In the following it is assumed, that the course of the process velocity is known a priori. Then the equation of motion of a single point can be solved:

$$z(t = t_0 + \Delta t) = z(t_0) + \int_{t_0}^{t_0 + \Delta t} v(\tau) d\tau \quad (15)$$

Here  $t_0$  is a point time for which the distribution of the state variables is known:  $\mathbf{x}(t = t_0, z) = \mathbf{g}(z)$  and  $\Delta t$  is a time step chosen much smaller than the residence time of a differential element in the domain of interest. In simulation, the inputs of the plant are held constant over the time period  $\Delta t$ . In order to determine the value of the state variables at the output location  $z = L$  and the point in time  $t = t_0 + \Delta t$ , one has to integrate the remaining characteristic ODEs with the appropriate initial conditions:

$$\mathbf{x}(t = t_0 + \Delta t, z = L) = \mathbf{g}(z(t = t_0)) + \int_{t_0}^{t_0 + \Delta t} \mathbf{f}(\mathbf{x}, z(\tau), \tau) d\tau \quad (16)$$

$z(t = t_0)$  is determined by setting  $z(t = t_0 + \Delta t)$  equal to  $L$  and then solving for  $z(t_0)$  in equation (15). The distribution of the state variables  $\mathbf{x}(t = t_0 + \Delta t, z = L - dz)$ ,  $\mathbf{x}(t = t_0 + \Delta t, z = L - 2 \cdot dz)$ ,  $\mathbf{x}(t = t_0 + \Delta t, z = L - 3 \cdot dz)$ , ... is determined by integrating the characteristic ODEs with initial conditions  $\mathbf{g}(z(t = t_0) - dz)$ ,  $\mathbf{g}(z(t = t_0) - 2 \cdot dz)$ ,  $\mathbf{g}(z(t = t_0) - 3 \cdot dz)$ , ... separately. Since all the points evolve completely uncoupled from each other, this can be performed with high accuracy. In practice, one is not able to integrate all of the  $\infty$  many sets of ODEs corresponding to the  $\infty$  many points, that can be found in the domain at the point in time  $t_0$ . Thus one is restricted to solve for a finite number of  $N$  points in the domain. In sequence the distribution of the state variables at the point in time  $t = t_0 + \Delta t$  can be interpolated using cubic splines or a linear interpolation scheme. Once the interpolation object is created from the state variables at time instant  $t_0 + \Delta t$  the simulation can proceed with time instant  $t_0 + 2 \cdot \Delta t$ . Now one has to update  $\mathbf{g}(z) := \mathbf{x}(t_0 + \Delta t, z)$  using the only recently created interpolation object. Note that when the process velocity is constant, one can always choose a time step  $\Delta t$  and a spacing  $s$ . t. interpolation is not necessary and thus the accuracy of the simulation is completely unaffected by the grid. In contrast, when Discretization on Finite Differences, Elements or Volumes is applied, the spacing has to be chosen small enough in order to fulfill accuracy requirements and numerical stability of the solution [4]. The main drawback of the classical lumping techniques lies in the fact, that these methods can not be used to simulate transient steps in the printing process. At a certain point in time, the sign of the process velocity  $v(t)$  switches and every point moves in the negative direction of the spatial variable, as one can see in figure 3. When the classical lumping techniques are used, at that point in time the boundary condition on the other end of the domain of interest ( $z = L$ ) must be supplied. By tracking a finite number of points along their Characteristic Curves one easily overcomes these difficulties.

**Remark.** In the model for the thermal fusing process, the initial condition  $\mathbf{g}(z)$  is defined for  $z \in \mathbb{R}$ , the points arrive at  $-\infty$  with constant temperature and moisture content. In the numerical treatment the point at which constant temperature and moisture content is found is chosen to be located at some finite distance upstream. The distance is chosen to be a multiple of the length  $L$  of the domain of interest. The state of that point and its position remains untouched  $\forall t$ . Similar, the points leave at  $+\infty$ , which in the numerical treatment is approximated by a multiple of the length  $L$  downstream.

## 5 Simulation of the Thermal Fusing Process

In the following the proposed method for simulation of nonlinear, time variant transport processes is applied to the thermal fusing process, which is described by the set of PDEs (7) subject to the initial conditions (8) and boundary conditions imposed at  $z = -\infty$  as described above. Initially, the system is assumed to be at steady state; the process velocity is equal to  $v(t) = v_s$ . The steady state distributions of temperature  $x_{1,s}(z)$  and moisture content



$x_{2,s}(z)$  are determined by setting the partial derivatives w.r.t time in the set of equations (7) equal to zero and solving the resulting set of ODEs. The temperature of the emitting surfaces  $u_i(t) = u_{i,s}, i = 1, \dots, 12$  is chosen, s.t. the plant output  $y(t) = y_s$  is equal to  $r$ . The profiles are displayed in figure 3. The process velocity over the time interval  $[0 \ t_c]$  takes the course as displayed in figure 3. In the printing process the course is repeated periodically: The cycle has a period equal to  $t_c$ . When the process velocity decays to zero and paper is pulled back, the curtain covers the hot emitting surfaces and prevents the paper web from being incinerated. The temperature of the emitting surfaces is left constant and equal to  $u_{i,s}, i = 1, \dots, 12$  during this transient step in the printing process. The timing of the curtain effects the distribution of temperature and moisture content in the domain  $\Omega \times [0 \ t_c]$ . The course of the plant input  $u_0(t)$ , which describes the position of the curtain is shown in figure 3. In figure 4 the distribution of temperature in the domain  $\Omega \times [0 \ t_c]$  is displayed for the nominal system (constant process parameters  $\varepsilon = \varepsilon^*, \beta = \beta^*, \alpha = \alpha^*$ ). One can see, that paper elements, that have already been cooled, eventually are pulled back into the fusing apparatus. This causes the outlet temperature to decrease. Before the emitting surfaces are completely covered by the curtain ( $u_0 = u_{min}$ ), radiant energy is continuously transferred. Thus, paper elements found at the beginning of the apparatus receive additional thermal energy. Toward the end of the printing cycle the paper is accelerated into the direction of processing and the process returns to the steady state again (see figures 3 and 4).

The control objective for the process is to maintain a desired outlet temperature  $T_d = r$ , when the velocity is equal to  $v_s$ . This implies, that the steady state outlet temperature is controlled by manipulating the temperature of the emitting surfaces  $u_i, i = 1, \dots, 12$ . From the projection of the Characteristic Curves into the  $[t \ z]$ -plane, displayed in figure 3, it becomes clear, that at  $t_c, 2 \cdot t_c, \dots, k \cdot t_c$  the steady state outlet temperature is measured at  $z = L$ . At these points in time, all the disturbances, resulting from the past break in processing, have completely settled in the domain of interest  $\Omega \subseteq \mathbb{R}$  (see figures 3). In the following two control laws, proportional (P) and proportional/integral (PI), are simulated assuming ideal actuators  $T_{E,i} = u_i(t), i = 1, \dots, 12$ . Since the objective is to maintain constant steady state outlet temperature, the sampling time for the control algorithm is equal to  $t_c$ . The steady state outlet temperature is measured, compared to  $r$  and proportional to the error  $e(k \cdot t_c) = r - x_1(k \cdot t_c, L)$  the emitter temperature is manipulated:

$$u_i(k \cdot t_c) = K_P \cdot e(k \cdot t_c), \quad i = 1, \dots, 12 \tag{17}$$

holds for the proportional controller and

$$u_i(k \cdot t_c) = K_P \cdot e(k \cdot t_c) + K_I \cdot \int_0^{k \cdot t_c} e(\tau) d\tau, \quad i = 1, \dots, 12 \tag{18}$$

holds for the controller with integral action. Note that the integral is converted into a sum for implementation.  $K_P$  and  $K_I$  are tuning parameters.

Disturbances of the process can be regarded as fluctuations in the process parameters, most of all the mass transfer coefficient  $\beta$  and the emission  $\varepsilon$  as defined in the system of equations (7).  $\beta$  depends on the quality of the paper web and  $\varepsilon$  is to a large extent affected by the population density of the toner on the surface of the web and the toner itself: Black toner absorbs more radiant energy than yellow toner. In the following the reaction of the closed loop to a step change in  $\varepsilon$  is studied. At  $t = 3 \cdot t_c$  the coefficient  $\varepsilon$  is raised by fifteen percent. This scenario describes a drastic change in population density of toner on the surface of the paper web. As a consequence, the surface absorbs more radiant energy and a lower emitter temperature  $u_i(t)$  is required to maintain a steady state outlet temperature  $y(k \cdot t_c) = r$ . The reaction of the closed loop to the disturbance is shown in figure 3 for both control laws given by equations (17) and (18). In the figure it can be noticed that the pure proportional controller does have a steady state offset while the controller with integral action manages to adjust the emitter temperature, s.t. the error decays to zero. In both cases the response of the closed loop is rather sluggish: It takes many printing cycles for the response to settle.

## 6 Conclusions

In this contribution a model for the spatiotemporal dynamics of the thermal fusing process in electro photographic printing has been derived. The process is a non linear, time variant transport process, described by two first order partial differential equations. The Method of Characteristics and the geometrical interpretation of a first order PDE is applied to simulate the plant output and the distribution of the state variables in the domain of interest. The simulation can be performed with high accuracy and little numerical effort. Difficulties associated with spatial discretization are avoided by tracking a finite number of points and their states (temperature and moisture content) along the Characteristic Curves, which are dictated by the course of the process velocity. The simulation allows the process engineer to study and improve the distribution of temperature in the domain of interest during transient operation of the process. The response of the closed loop to a step change in one of the important process parameters has been studied. Although optimal tuning of the tuning parameters of the proportional/integral controller may improve the response, it is expected, that the response of the closed loop can

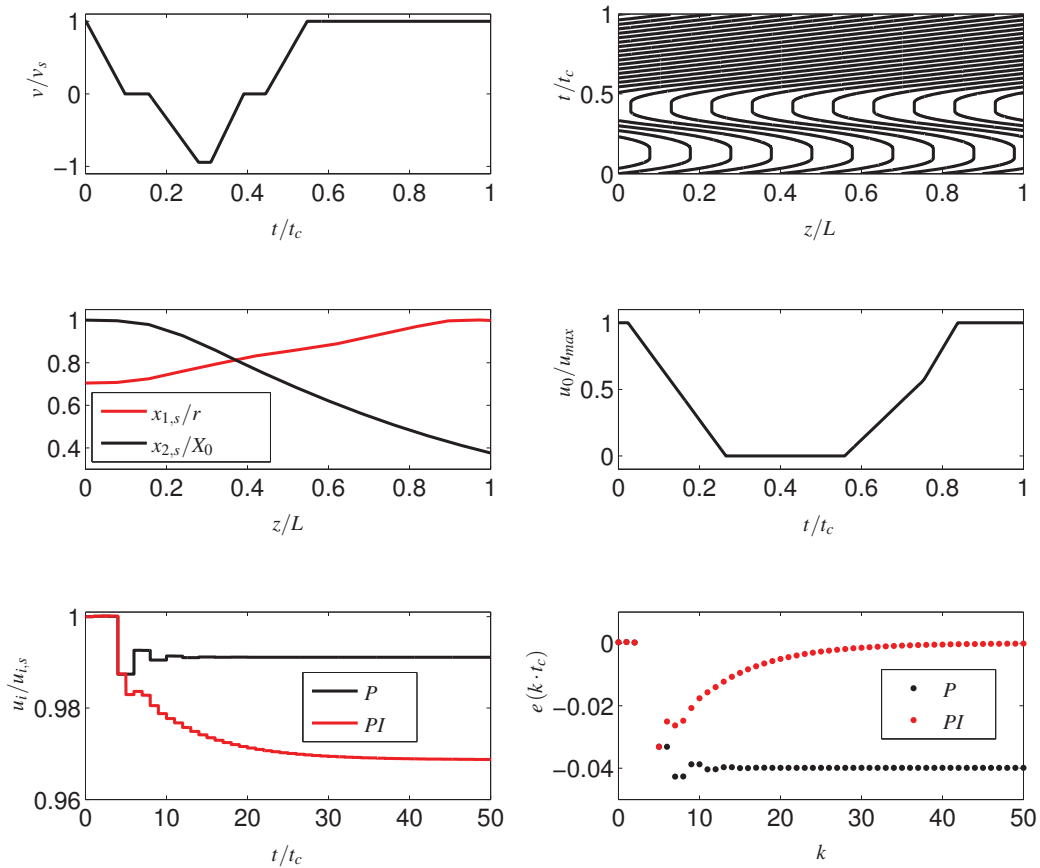


**Figure 3:** Upper Left: Course of process velocity. Upper Right: Projection of the Characteristic Curves in the thermal fusing process into the domain of interest. The trajectories shown above can be interpreted as the solution of the equation of motion for some of the  $\infty$  many points traveling through the domain of interest. Center left: Steady state distribution of temperature and moisture content. Center right: The course of the plant input  $u_0(t)$ , which describes the position of the curtain. Lower left: Course of the temperature of the emitters  $T_{E,i} = u_i(t)$ ,  $i = 1, \dots, 12$ . Lower right: Course of the error; a change in the process parameter  $\varepsilon$  occurs at  $t = 3 \cdot t_c$ ,  $\varepsilon$  is increased by fifteen percent. As a consequence, the paper web absorbs more radiant energy and leaves the domain of interest with a larger temperature than desired.

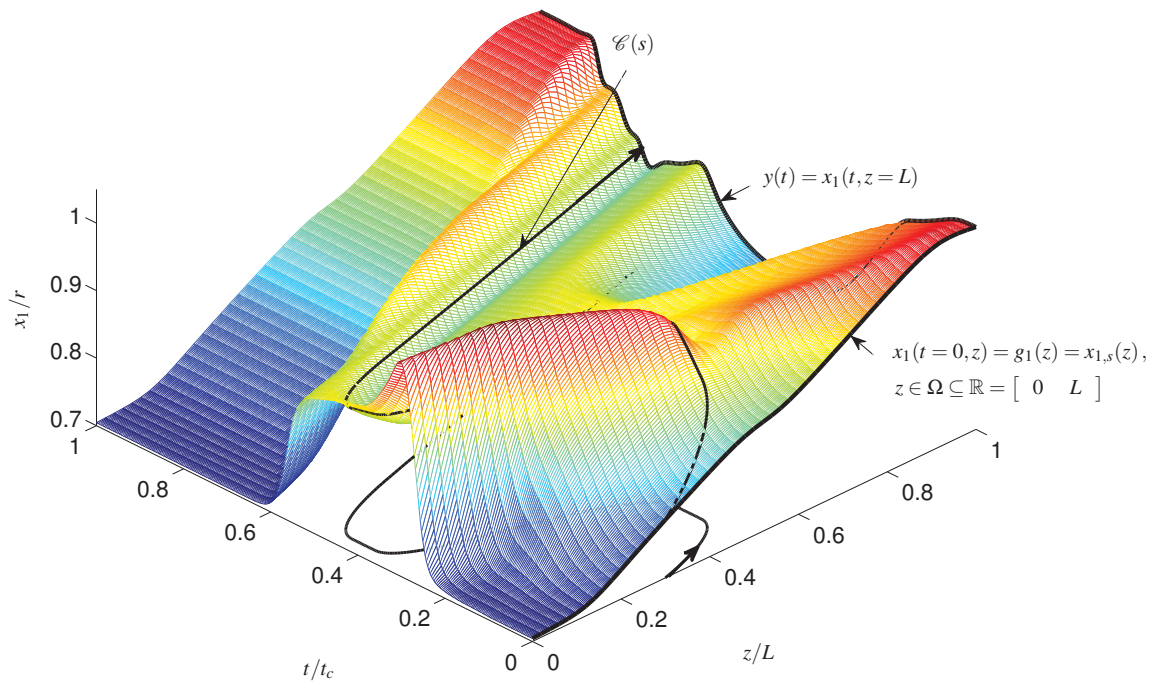


**Figure 4:** Solution surface for the temperature of the paper web  $x_1$  in the domain  $\Omega \times [0 t_c]$ . Also shown in the figure is a single Characteristic Curve  $\mathcal{C}(s)$  and the projection into the  $[t z]$ -plane. One can see, how the temperature evolves along that curve. The initial conditions for the Characteristic ODEs (14) are:  $t(s=0) = 0$ ,  $z(s=0) = 0.3 \cdot L$  and  $\mathbf{x}(s=0) = \mathbf{g}(0.3 \cdot L)$ . Eventually the curve arrives at the sensor location  $z=L$  and the temperature  $x_1$  at that particular point on the Characteristic Curve is equal to the plant output at that point in time.

be significantly enhanced by online parameter estimation (estimation of  $\beta$ ,  $\varepsilon$  and  $\alpha$ ) and feedforward control of the emitter temperature [10]: Based on the current estimation of the parameters, the emitter temperature, which is required for the steady state output  $y(k \cdot t_c)$  to be equal to  $r$ , can be taken from a look-up table and fed forward to the control algorithm.

## 7 References

- [1] R. B. Bird. *Transport phenomena*. Wiley, New York, 2002.
- [2] P. D. Christofides. *Nonlinear and Robust Control of PDE Systems*. Birkhäuser, Boston, 2001.
- [3] L. Debnath. *Nonlinear Partial Differential Equations for Scientists and Engineers*. Birkhäuser, Boston, 2nd Ed., 2005.
- [4] J. H. Ferziger. *Computational Methods for Fluid Dynamics*. Springer, New York, 3rd. Ed., 2002.
- [5] G. Goldmann. *Digital Printing*. OCE Printing Systems, Poing/Munich, 9th Ed., 2005.
- [6] F. P. Incropera. *Fundamentals of Heat and Mass Transfer*. Wiley, New York, 6th Ed., 2006.
- [7] W. S. Janna. *Engineering Heat Transfer*. PWS Engineering, Boston, 1986.
- [8] R. B. Keey. *Drying: Principles and Practice*. Pergamon Press, New York, 1972.
- [9] A. Mersmann. *Thermische Verfahrenstechnik: Grundlagen und Methoden*. Springer, Berlin, 2nd Ed., 2005.
- [10] S. Studener. *Estimation of Process Parameters on a Moving Horizon for a Class of Distributed Parameter Systems*. -, submitted to the Journal of Process Control, 2008.
- [11] E. M. Williams. *The Physics and Technology of Xerographic Processes*. Wiley, New York, 1984.



Property	Comment	Unit
$A$	Constant of the equilibrium moisture content	$K^{-1}$
$c_P$	Heat capacity of paper	$J \cdot kg^{-1} \cdot K^{-1}$
$D$	Diffusion coefficient of water	$m^2 \cdot s^{-1}$
$d_P$	Thickness of paper web	$m$
$e$	Error	$K$
$H$	Distance above paper web	$m$
$K_I$	Constant of the control algorithm	$s^{-1}$
$K_P$	Constant of the control algorithm	—
$L$	Length of apparatus	$m$
$L_{Emitter}$	Length of emitter	$m$
$\Delta L_1$	Spacing	$m$
$\Delta L_2$	Spacing	$m$
$r$	Set point or control objective	$K$
$s$	Parameter of Characteristic Curve	—
$T_d$	Desired outlet temperature	$K$
$T_{env}$	Environmental temperature in the apparatus	$K$
$T_P$	Temperature of paper	$K$
$T_0$	Temperature of paper before the apparatus	$K$
$T_\infty$	Environmental temperature	$K$
$t$	Time	$s$
$t_c$	Processing time	$s$
$u_0 = u$	Plant input: Curtain position	$m$
$u_i$	$i = 1, \dots, 12$ , Plant input: Emitter temperature	$K$
$v$	Process velocity	$m \cdot s^{-1}$
$v_s$	Steady state process velocity	$m \cdot s^{-1}$
$W_{Emitter}$	Width of emitter	$m$
$W_{Paper}$	Width of paper	$m$
$\Delta W$	Spacing	$m$
$X_0$	Nominal moisture content of paper	—
$X$	Moisture content	—
$x_1$	State variable: Temperature	$K$
$x_2$	State variable: Moisture content	—
$y$	Plant output	$K$
$z_1$	Spatial variable	$m$
$z_2$	Spatial variable	$m$
$z_{E,1}$	Spatial variable	$m$
$z_{E,2}$	Spatial variable	$m$
$\alpha$	Coefficient for convective heat exchange (in Eq. (7))	$s^{-1}$
$\beta$	Coefficient for mass transfer (in Eq. (7))	$s^{-1}$
$\varepsilon$	Coefficient for radiant heat exchange (in Eq. (7))	$s^{-1} \cdot K^{-3}$
$\varepsilon_E$	Emission of emitter	—
$\varepsilon_P$	Emission of paper	—
$\lambda_P$	Thermal conductivity of paper	$W \cdot m^{-1} \cdot K^{-1}$
$\rho_P$	Density of paper	$kg \cdot m^{-3}$
$\sigma$	Stefan Boltzmann Number	$W \cdot m^{-2} \cdot K^{-4}$

**Table 1:** List of symbols. For reasons of concealment, numerical values of the physical properties can be provided upon approval by OCE Printing Systems and after correspondence with the author.